

Supplement of Atmos. Chem. Phys., 17, 12597–12616, 2017
<https://doi.org/10.5194/acp-17-12597-2017-supplement>
© Author(s) 2017. This work is distributed under
the Creative Commons Attribution 3.0 License.



Supplement of

Multi-source SO₂ emission retrievals and consistency of satellite and surface measurements with reported emissions

Vitali Fioletov et al.

Correspondence to: Vitali Fioletov (vitali.fioletov@outlook.com, vitali.fioletov@canada.ca)

The copyright of individual parts of the supplement might differ from the CC BY 3.0 License.

S1. The bias and residuals

As discussed in the Appendix, the first term in equation A4 is the emission-related fitting results and second term represents the large-scale bias. Figure S1 shows the differences between the actual OMI VCD data and the emission-related fitting results plus the bias (ϵ from equation A4 labeled as “Residual 1”), the estimated bias itself, and the difference between the fitting results and the VCDs calculated directly from the emissions inventories (Residual 2). As Figure S1 (middle column) demonstrates, the bias values are consistent over time and elevates SO_2 values over the U.S. East Coast and its magnitude is typically within ± 0.1 DU.

SO_2 VCD data from the Ozone Mapping Profiler Suite (OMPS) Nadir Mapper on board the Suomi National Polar-orbiting Partnership (or Suomi NPP) satellite operated by NASA/NOAA and launched in October 2011 were also used in the study to verify a potential bias in some OMI data. OMPS data were processed with the same PCA algorithm as OMI data (Li et al., 2013). OMPS has a lower spatial resolution than OMI, 50 km by 50 km, but better signal-to-noise characteristics. The comparison of OMI and OMPS data shows that the bias is present in OMI data but not in OMPS. Figure S2a shows OMI mean SO_2 for 2013-2015, the estimated bias, OMI data with the bias removed and the mean OMPS SO_2 for the same period. OMI maps with the bias removed demonstrate a good agreement with the OMPS map, while the original OMI data have elevated values along the US East Coast, particularly over eastern North and South Carolina. The largest bias occurs in winter month as also illustrated by Figure S2b.

The reason for the bias is not well understood. However, the difference between OMI and OMPS data, both processed with the PCA algorithm, suggests that at least some of the bias is of instrumental origin. Incorrect retrieval assumptions could also be contributors. Two possibilities here are surface reflectivity and assumed ozone profiles. Since this bias has a seasonal-dependence, a third possibility is a small mismatch between the measurement conditions and the conditions under which the principle spectral components were derived.

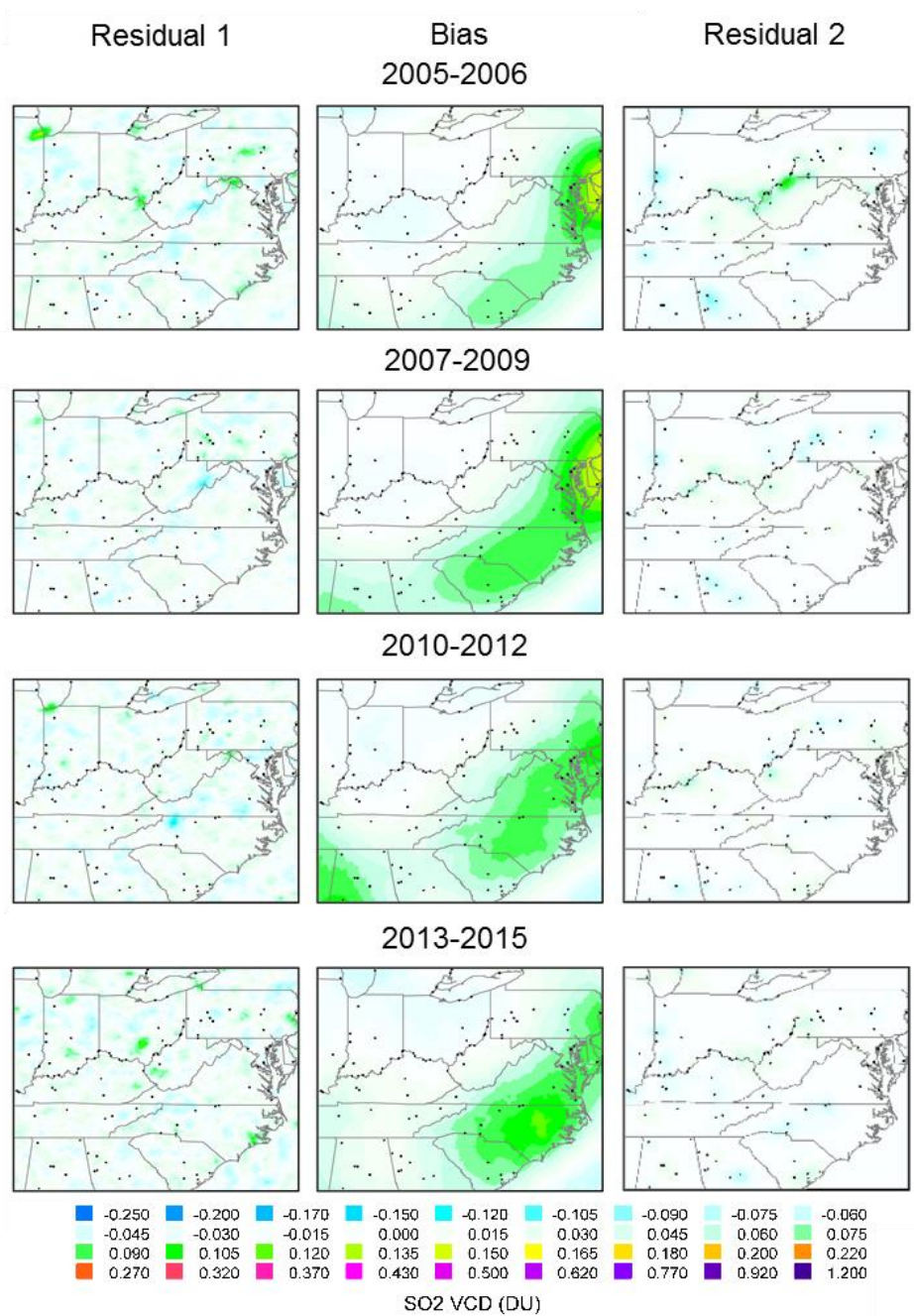


Figure S1. The differences between the actual OMI VCD data and the emission-related fitting results plus the bias (Residual 1), the estimated bias itself, and the difference between the fitting results and the VCDs calculated directly from the emissions inventories (Residual 2) for four time periods.

If the analyzed area is small, say a few hundred km by a few hundred km, we can simply assume a constant bias. However, for large areas, this assumption does not work and we instead add a polynomial function that changes relatively slowly with latitude and longitude. The required polynomial degree depends on the area size and the gradients of that slowly changing bias.

The bias estimated using polynomials of 0, 2, 4, and 6th degree is shown in Figure S3. Note that the bias is estimated for every season separately and then the average bias over the entire period was calculated. Due to different sampling, the overall bias is not constant even if a constant (0-degree polynomial) is used. While there is a noticeable difference between the biases estimated using a constant function or 2nd-degree polynomial and the bias based on a 4th-degree polynomial, further increases of the polynomial degree do not change the results very much.

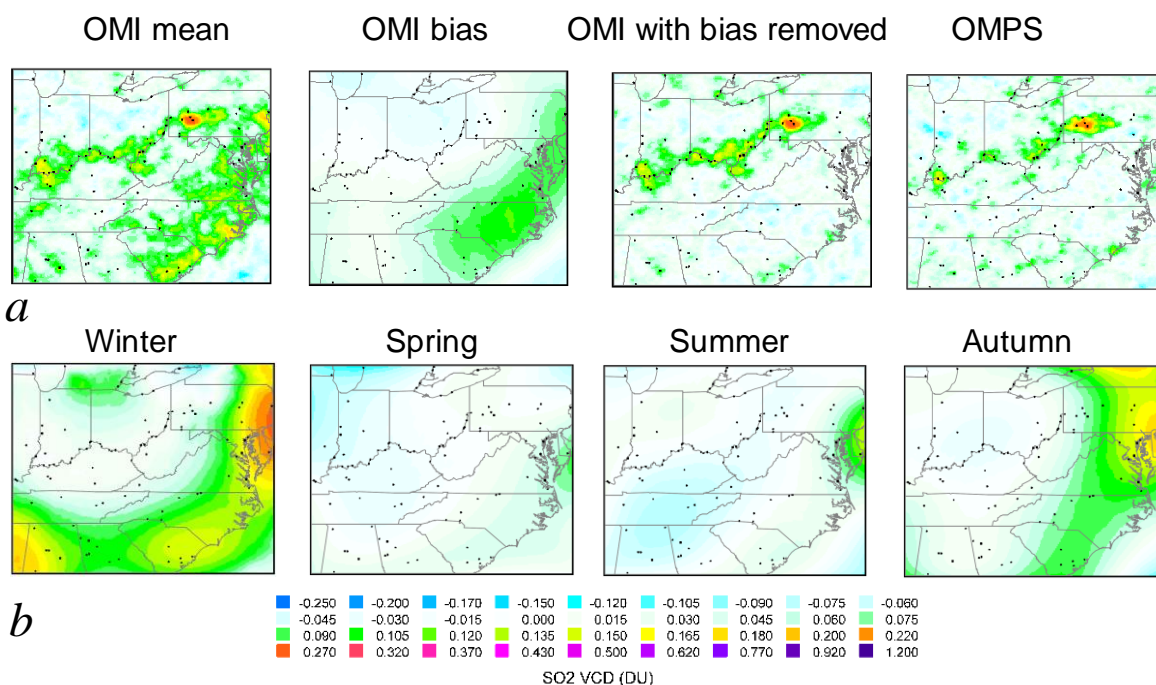


Figure S2. (a) OMI and OMPS SO₂ VCD data for 2013-2015. The mean OMI values, the estimated OMI large-scale bias, the mean OMI values with the bias removed and the mean OMPS values are shown. (b) Large scale biases estimated from OMI 2005-2006 data for different seasons

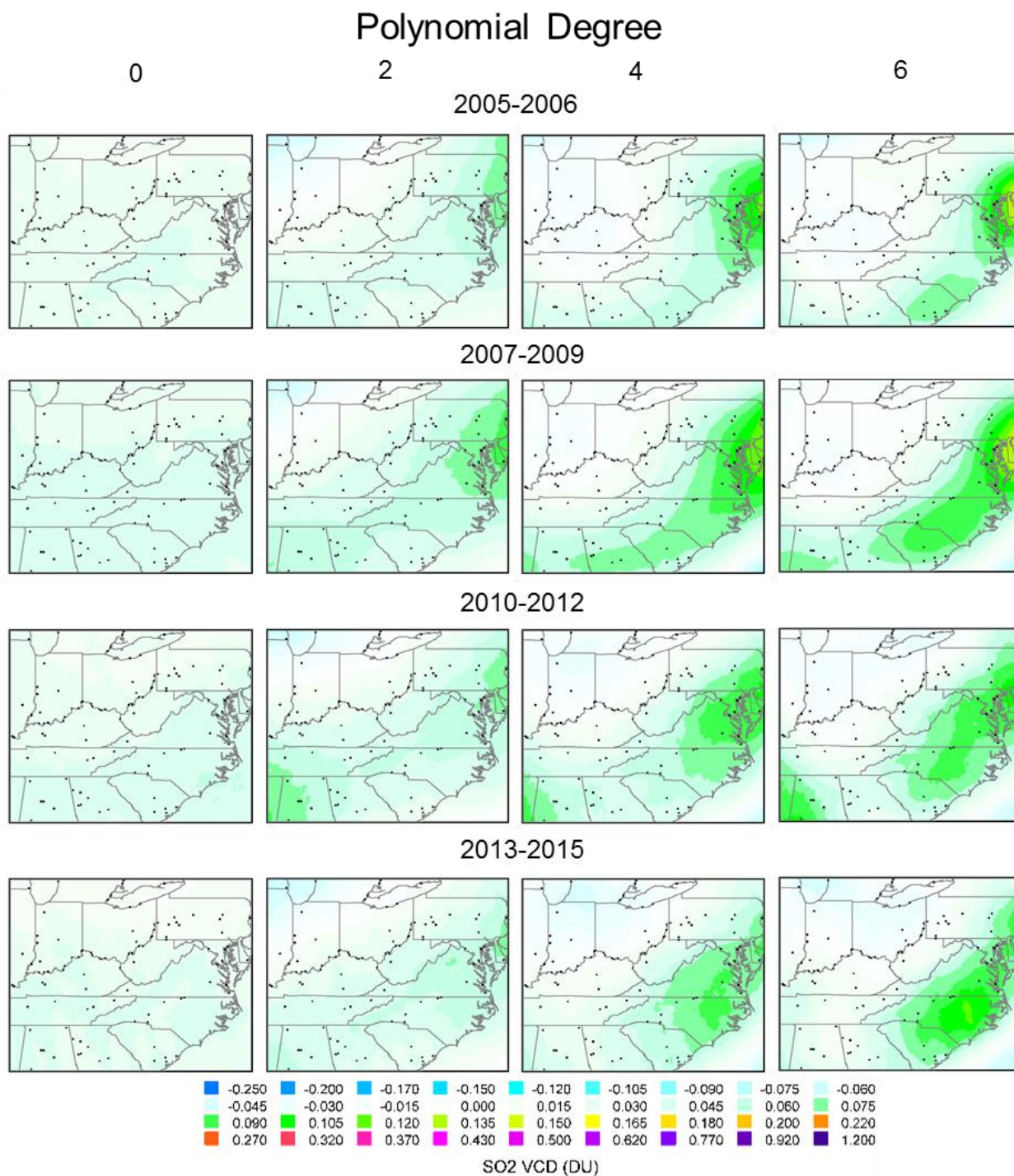


Figure S3. The large-scale biases estimated using polynomials of 0, 2, 4, and 6th degree.

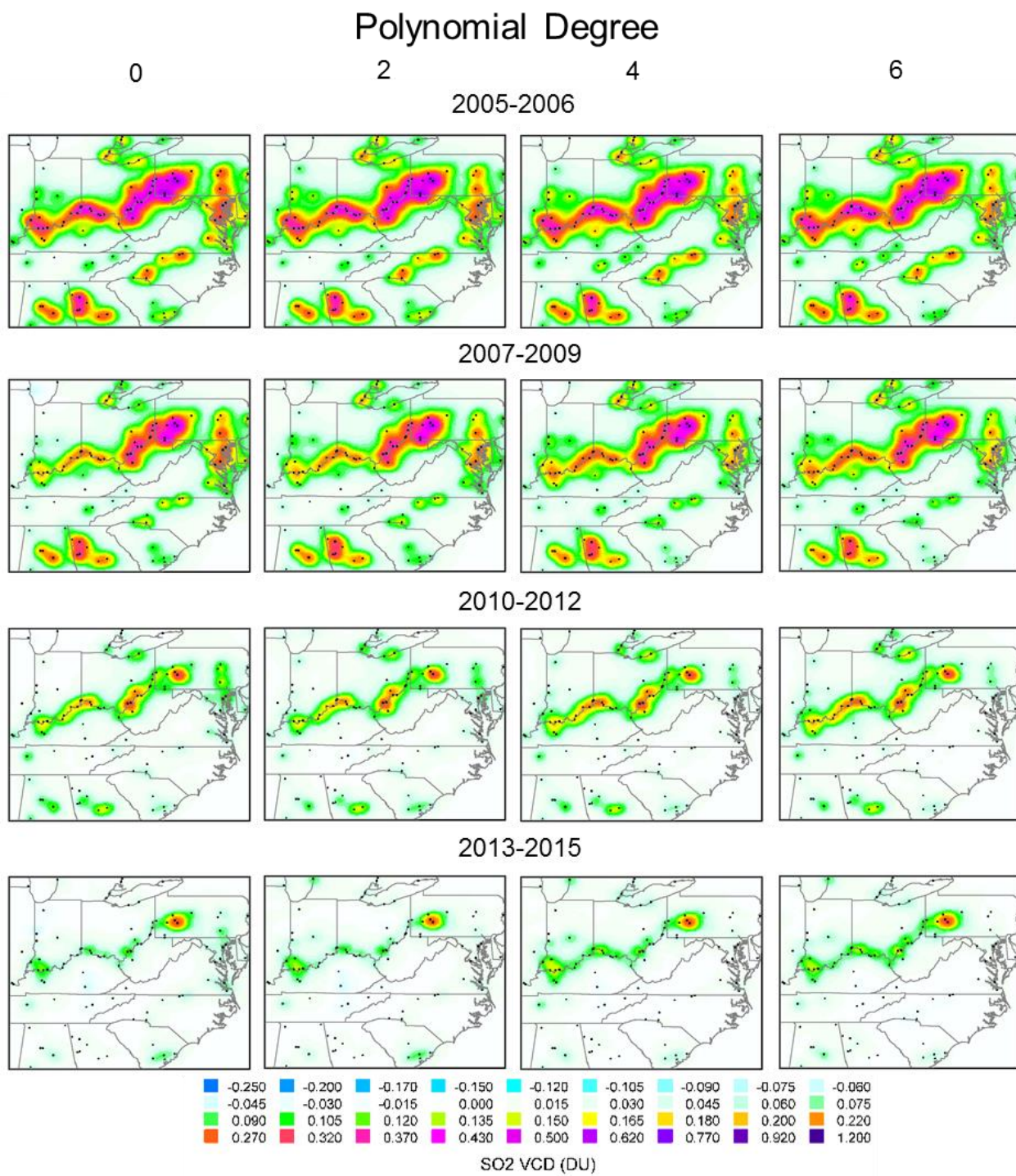


Figure S4. Results of the fitting of OMI data by the set of functions that represent VCDs near emission sources using estimated emissions (the same as column III in Figure 1) for polynomials of 0, 2, 4, and 6th degree used to fit the bias.

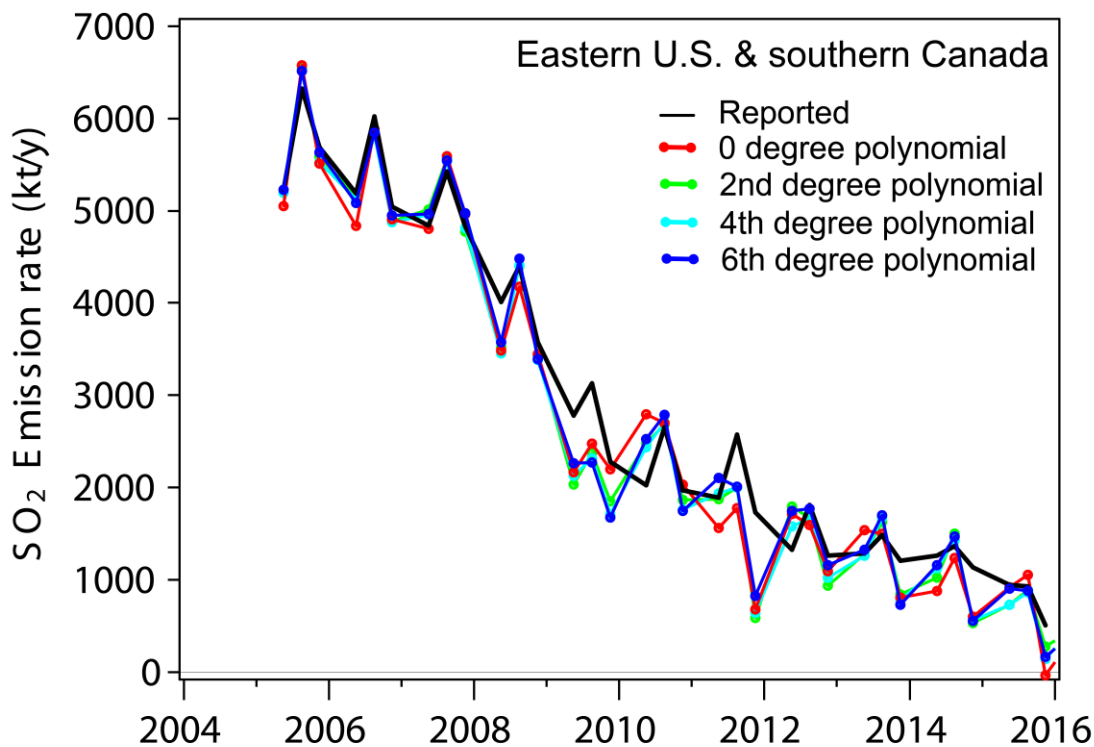


Figure S5. Reported and estimated seasonal point-source emissions rates for the entire eastern U.S. and southeastern Canada (the region shown in Figure 1) for spring, summer, and autumn for different degrees of the polynomial fit. Estimated emissions are shown for the statistical model based on the actual source location and different colors represent different polynomial degrees of the fitting function. As in Figure 2, the seasonal emissions values are scaled to give annual emission rates. Winter data are not shown due to high uncertainties of the OMI measurements.

The fitting results themselves are shown in Figure S4. The fitting results, i.e., SO₂ VCDs derived from estimated emissions using the actual wind data, show little dependence on polynomial degree, suggesting that the emission estimates themselves are not very sensitive to the degree of the polynomial fit.

Figure S5 (similar to Figure 2d) shows the estimated emissions themselves for the entire eastern U.S. and southeastern Canada (the region shown in Figure 1 and in Figures S1-S4) for spring, summer, and autumn. The emission estimates for the entire region are very similar for all presented polynomial fits, i.e., the degree of the fit does not play a major role, at least, in that particular region.

Figure 3 shows the scatter plots between the annual VCDs reconstructed from emissions and the three OMI-based data sets shown in Figure 1 (columns (I-III) for all years as well as the correlation coefficients between the two data sets on each plot. These correlation coefficients can be used to find the optimal degree of Legendre Polynomials used to remove the large-scale bias. The correlation coefficient between OMI data with bias removed and VCDs calculated from the emission data is 0.75 for the actual OMI data, and 0.80, 0.83, 0.87, 0.89, 0.90, 0.909 for the bias removed by the 1st, 2^d, 3^d, 4th, 5th, and 6th degree polynomials respectively. The correlation noticeably improved if the polynomial bias removed, but the improvement is only marginal for the degrees above 4.

S2. Seasonal and annual statistics

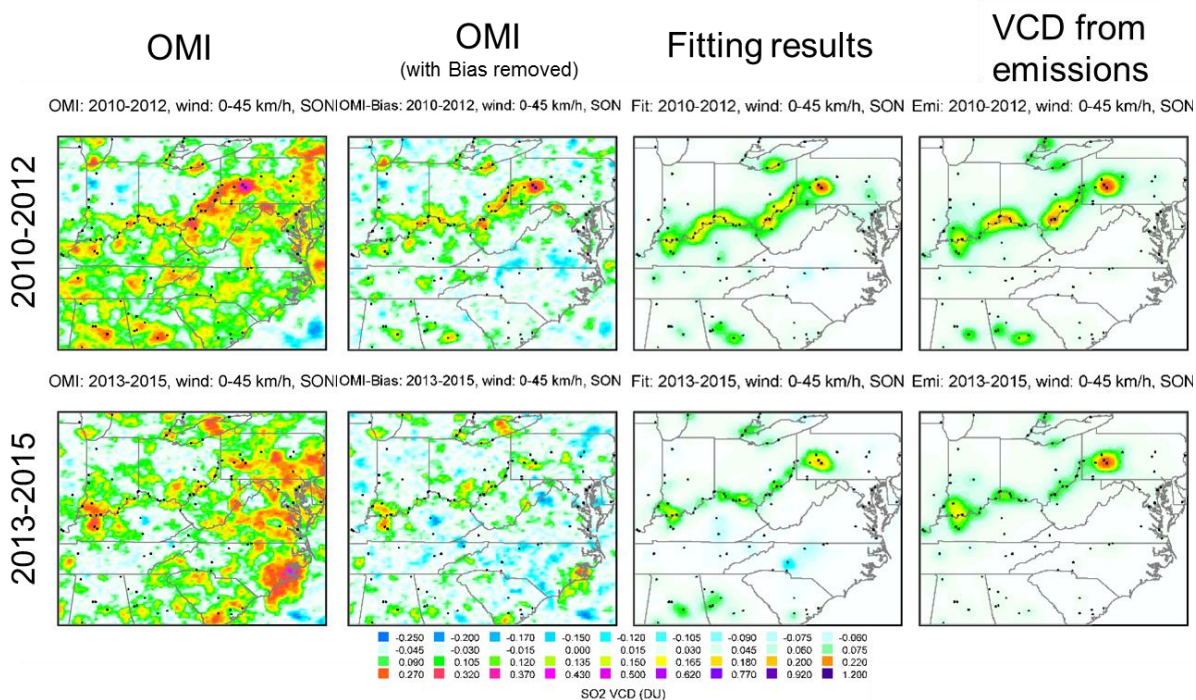


Figure S6. Autumn mean OMI SO₂ VCDs, mean OMI SO₂ VCDs with a large-scale bias removed, results of the fitting of OMI data by the set of functions that represent VCDs near emission sources using estimated emissions (see the paper text), and SO₂ VCDs calculated using the same set of functions but using reported emission values. Averages for 2010-2012 and 2013-2015 are shown. Sources that emitted 20 kt yr⁻¹ at least once in 2005-2015 were included in the fit (they are shown as the black dots).

Table S1. The correlation coefficients between SO₂ VCDs estimated from the reported emissions and OMI data, OMI data with local bias removed, and the results of fitting OMI data. The data were averaged over 1° by 1° grid cells.

Season*	OMI data	OMI data with bias removed	Fitting results
All grid cells			
Winter (1731)	0.17	0.24	0.70
Spring (1815)	0.60	0.75	0.93
Summer (1815)	0.80	0.88	0.96
Autumn (1815)	0.54	0.72	0.91
Year (1815)	0.75	0.91	0.97
Only cells with OMI SO ₂ values greater than 0.1 DU			
Winter (1060)	0.13	0.28	0.83
Spring (441)	0.72	0.84	0.95
Summer (410)	0.82	0.91	0.96
Autumn (882)	0.61	0.81	0.94
Year (570)	0.84	0.96	0.98

*The number of cells is shown in brackets

Table S2. The correlation coefficients between SO₂ VCDs estimated from the reported emissions and OMI data, OMI data with local bias removed, and the results of fitting OMI data for different years. The data were averaged over 1° by 1° grid cells.

Year	OMI data	OMI data with bias removed	Fitting results
2005	0.91	0.96	0.99
2006	0.84	0.95	0.98
2007	0.86	0.96	0.99
2008	0.76	0.92	0.98
2009	0.57	0.85	0.97
2010	0.59	0.84	0.95
2011	0.34	0.73	0.95
2012	0.29	0.73	0.91
2013	0.28	0.69	0.86
2014	0.18	0.62	0.89
2015	0.25	0.57	0.83

The correlation coefficients between SO₂ VCDs estimated from the reported emissions and OMI data, OMI data with local bias removed, and the results of fitting OMI data for individual seasons (all years) and for individual years (all seasons) are shown in Tables S1 and S2 respectively. The data were averaged over 1° by 1° grid cells. The seasonal correlation coefficients are the highest in summer and the lowest in winter in line with the uncertainties of OMI measurements. The correlation coefficients with the actual OMI data are lower than with the data with bias removed as expected from Figure S2 because the bias is comparable with the signal itself in recent years. For the OMI actual data, a large fraction of all cells have SO₂ levels close to the noise level. Excluding these cells from the statistics by putting a limit for SO₂ be greater than 0.1 DU increases the correlation coefficients. The correlation coefficients declined with time as expected from the decline in emissions and therefore in the signal-to-noise ratio.

There are very high correlation coefficients between all four data sets in 2005 when the signal was relatively high and the noise was relatively low due to a large number of pixels (as OMI data were not affected by the row anomaly). As the emissions decline with time, the correlation coefficients between OMI data and the estimated from emissions VCDs also decline. However, the correlation coefficients of the latter with the fitting results remained high, about 0.86 for 2013-2015, while the correlation coefficient with OMI data was only about 0.24 (Table S2). The fact that the correlation coefficients with OMI measurements were high for a strong signal suggests that the VCD calculations from emissions were able to accurately reproduce the SO₂ VCD distribution at that time. The uncertainties of VCD calculations from emissions do not really depend on the emission strength suggests that VCDs estimated from emissions remain accurate even in the recent years. Therefore, high correlation coefficients of these data with the fitting results means that the fitting procedure correctly extracts emission-related signal from noisy OMI data of the recent years. This could be used for OMI data analysis in other regions.

S3. Fitting results for individual seasons: autumn

Most of the results presented in the paper are based on annual means. It is possible to calculate 3-month seasonal statistics, although the results will generally be less reliable as the sample size is about four times smaller. According to Table S1, winter OMI data have practically no correlation with the emission-based SO₂ due to high noise level in OMI data and large number of rejected OMI pixels because of low sun elevation and snow on the ground. For the other seasons the correlation coefficients with emission-based SO₂ estimates are much higher, particularly for the fitting results. Figure S6 demonstrated how a relatively weak SO₂ signal for autumn in recent years can be extracted from the OMI measurements.

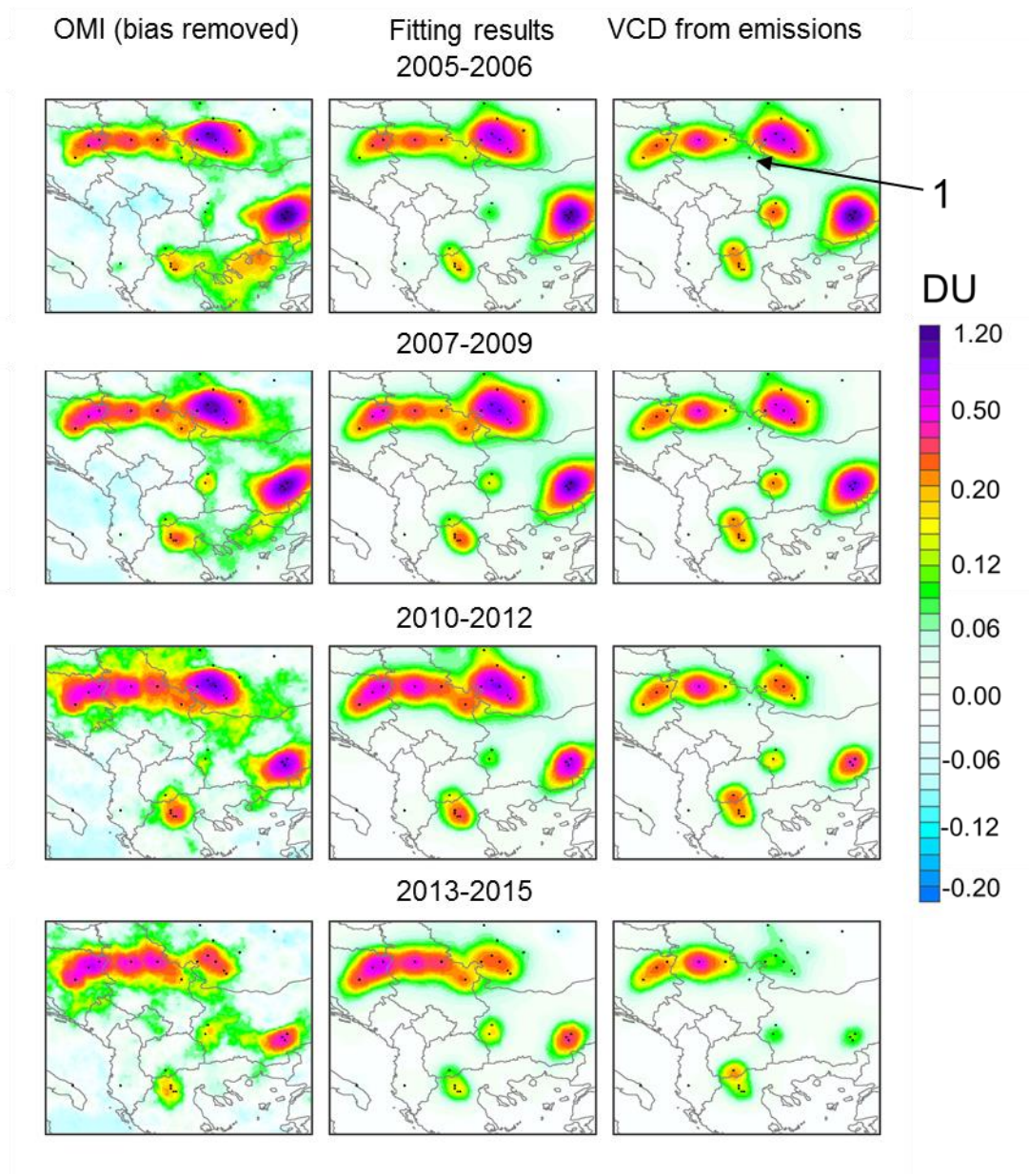


Figure S7. Annual mean OMI SO₂ VCDs over southeastern Europe with a constant large-scale bias removed (column 1), results of the fitting of OMI data by the set of functions that represent VCDs near emission sources using estimated emissions (column 2), and SO₂ VCDs calculated using the same set of functions but using reported emission values (column 3). Point sources that emitted 10 kt yr⁻¹ at least once in the period 2005–2015 were included in the fit (shown as black dots). The maps are smoothed by the pixel averaging technique with a 30 km radius (Fioletov et al., 2011). Averages for four multi-year periods, 2005–2006, 2007–2009, 2010–2012, and 2013–2015, are shown. The location of the Serbian smelter at Bor is indicated by “1”.

S4. SO₂ VCD over southeastern Europe.

Figure S7 is a “zoomed-in” version of Figure 5 that shows OMI data, the fitting results, and SO₂ VCDs estimated from emissions over a part of southern Europe. As shown in Figure S4, SO₂ sources in Serbia and Bosnia-Herzegovina are the largest remaining in Europe. Their emissions are not included in E-PRTR and TNO-MACC-III emission inventory data (see Section 2.3) were used in Figure S7 instead. While there is general agreement between VCDs from TNO-MACC-III emissions for Serbia and for Bosnia-Herzegovina, there are some discrepancies. In particular, based on the TNO-MACC-III inventory data, the high SO₂ values over the Serbian copper smelter at Bor, particularly from 2007–2012, are unexpected. OMI data from Figure S7 also show that SO₂ signals from large power plants in Romania and Bulgaria are not declining as rapidly as expected from the E-PRTR emissions inventory.

S5. SO₂ surface concentrations and VCDs

Figure S8 is similar to Figure 9d and shows the surface-concentration-to-column ratio as a function of the mean VCD. Unlike Figure 9, where the ratios were calculated from the slope of the regression lines and emission-based VCDs, the ratios in Figure S8 were calculated from 3-year averages (2005–2007) of measured surface concentrations and OMI SO₂ VCD values. In addition to CASTNet data used in the study (Figure 9a), the same analysis was done using data from the US AirNow network (<https://www.airnow.gov/>) and the results are shown in Figure S8b.

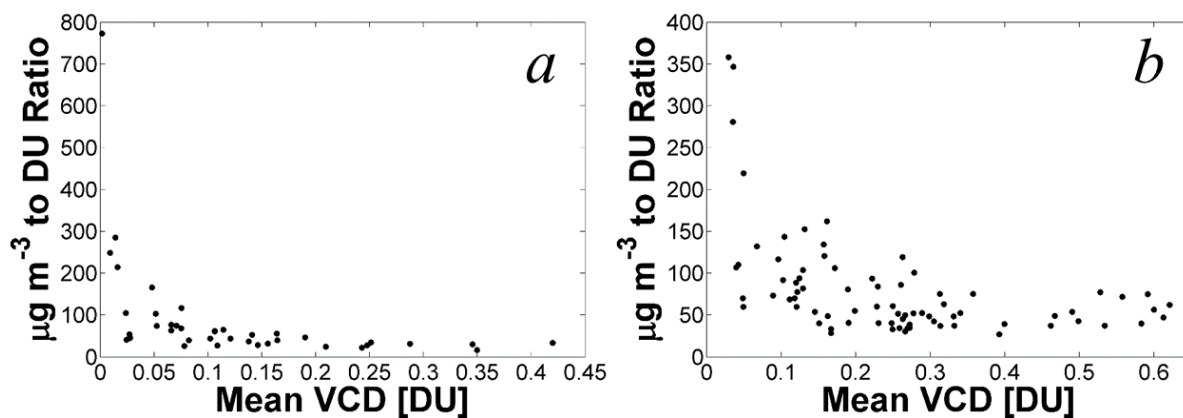


Figure S8. The site-specific surface-concentration-to-column ratio as a function of the 2005–2007 mean OMI SO₂ VCD. Each dot represents one site. Surface concentration data from the CASTNet (a) and AirNow (b) surface monitoring networks were used for the plot.

S6. Reconstructing the past VCDs using different wind data.

As mentioned in section 2.2, the actual OMI pixel locations and wind data for 2005 were used to reconstruct annual mean VCD maps based on annual reported emissions (section 3.4) for all years prior to 2005. To study the sensitivity of the results to a particular year (2005) of wind data, we repeated the calculations using 2006 wind data. Figure S9 is similar to Figure 7 and shows annual mean SO₂ VCD calculated using the reported emissions data and pixel locations and wind data for 2005 (top) and 2006 (bottom). Annual mean wind characteristics do not vary much from year to year and the reconstruction results for 2005 and 2006 winds are nearly identical.

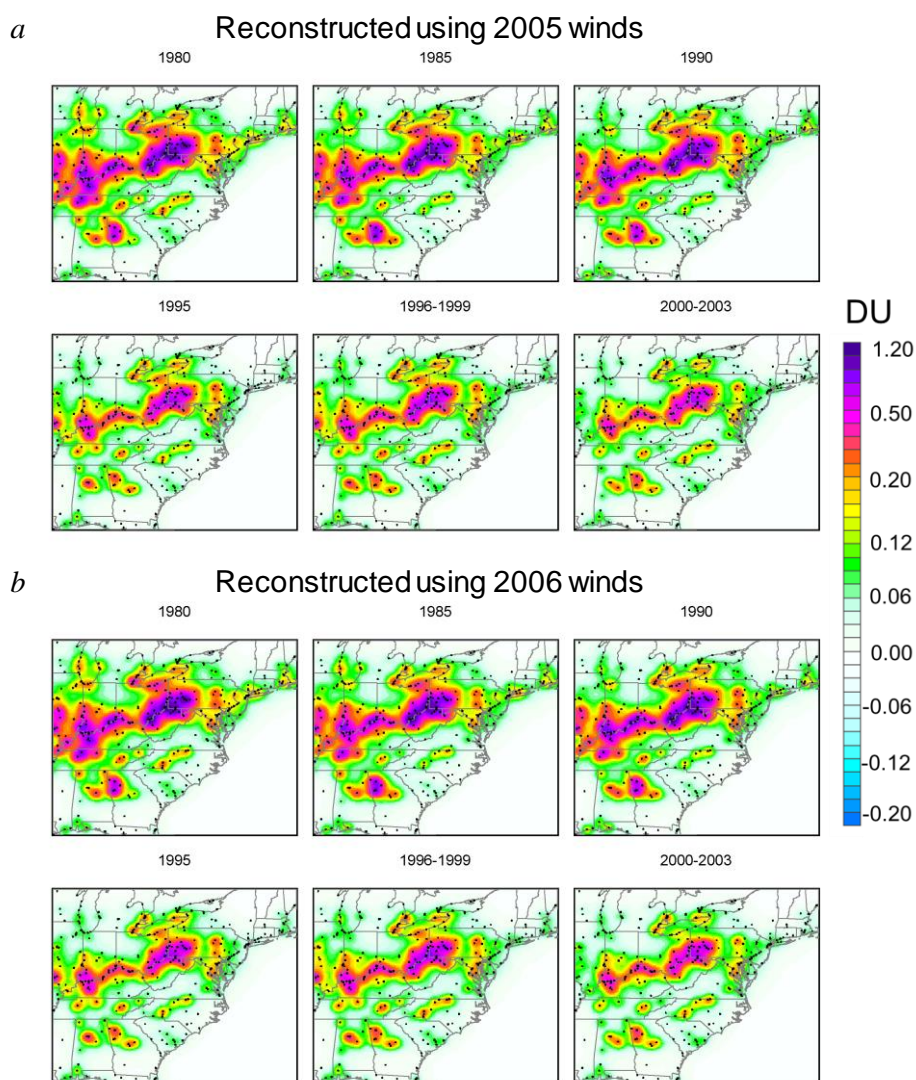


Figure S9. Annual mean SO₂ VCD calculated using the plume model applied to the reported emissions data for the period 1980-2003 calculated using the reported emissions data and pixel locations and wind data for 2005 (top) and 2006 (bottom).

References

Fioletov, V. E., McLinden, C. A., Krotkov, N. A. and Li, C.: Lifetimes and emissions of SO₂ from point sources estimated from OMI, *Geophys. Res. Lett.*, 42, 1–8, doi:10.1002/2015GL063148, 2015.

Li, C., Joiner, J., Krotkov, N. A. and Bhartia, P. K.: A fast and sensitive new satellite SO₂ retrieval algorithm based on principal component analysis: Application to the ozone monitoring instrument, *Geophys. Res. Lett.*, 40(23), 6314–6318, doi:10.1002/2013GL058134, 2013.